Optical and Quantum Electronics (2005) 37:1385–1395
DOI 10.1007/s11082-005-4218-1

Controllability of non-contact cell manipulation by image dielectrophoresis (iDEP)

YEN-SHENG LU[1], YUAN-PENG HUANG[1,*], J. ANDREW YEH[1], CHENGKUO LEE[2] AND YU-HUA CHANG[1]
[1]*Institute of Microelectromechanical Systems, National Tsing Hua University, No.101, Sec.2 Kuang-Fu Rd, Hsinchu 300, Taiwan*
[2]*Asia Pacific Microsystems, Inc., No. 2. R&D Rd. VI, Science-based Industrial Park, Hsinchu 300, Taiwan*
*(*author for correspondence: E-mail: g936203@oz.nthu.edu.tw)*

Received 2 February 2005; accepted 15 September 2005

Abstract. The controllability of cell manipulation using image dielectrophoresis (DEP) was characterized regarding DEP affinity test of cells, effective DEP radius, threshold voltage and parallel manipulation. The reconfigurable electrodes for DEP were achieved using an optically addressable projection array of 800 by 600. Each optical pixels projected on the chips were measured to be 25 μm by 25 μm. Individual pixels were controlled through a computer using a mouse cursor or pre-programmed flashes as projection patterns over a period of time. Based on the result of the DEP affinity test, effective DEP radius and threshold voltages, the parallel manipulation of cells without interfering each other was demonstrated.

Key words: cell manipulation, conductivity, controllability, image dielectrophoresis, non-contact

1. Introduction

In the last decade, there are extensive developments for cell manipulation technologies that contribute toward biological research and disease diagnose. These manipulation techniques for cell manipulation, separation, sorting and guidance can be divided into two categories, including direct contact and non-contact methods. The direct contact methods usually refer to mechanical manipulations using micropipettes or microgrippers (Wu *et al.* 1998; Edwin 2000). Microgrippers typically have small working distances and use electric energy or thermal energy to drive actuation. One microgripper is designed to be used for manipulation of one cell. Thus, such direct contact approaches are not feasible for applications in manipulation of a large amount of cells.

On the other hand, non-contact methods that utilize optical or electric energies to guide cells include optical tweezers (Ashkin *et al.* 1971, 1986, 2000), conventional dielectrophoresis (cDEP) (Pohl 1951, 1978; Wang *et al.* 1993, 1995; Yang *et al.* 1999; Sachiko 2001; Li *et al.* 2002; Das *et al.*

2005) and optically induced dielectrophoresis (Chiou *et al.* 2003; Lu *et al.* 2004a, b), etc. Optical tweezers use high gradient of optical pressure to guide cells by focusing a laser beam through a high N.A. lens on the cells. High optical intensity of about 10^{10} mW/cm^2 may cause damage on the cells; thus, optical tweezers are not suitable for long-term manipulation of cells (Neuman *et al.* 1998).

The DEP methods use the gradient of the electric energy applied to drive cells. The non-uniform electric fields are generally produced by spatially distributed electrodes. The electrodes are fabricated using microsystem fabrication technologies with masks to patterns physical geometry of the electrodes. In addition to physically patterned electrodes, the non-uniform fields can be also optically induced with photoconductive layers inserted between parallel electrodes. The parallel electrodes form uniform electric fields in between under bias applied. The electric fields become locally enhanced when the photoconductive layers have higher conductivities under illumination. This optical method was first demonstrated using laser as a light source to manipulate particle or cell (Chiou *et al.* 2003).

Alternative optical method was later developed using image projectors to simultaneously manipulate more cells over a wide range of areas (Ohta *et al.* 2004). The images projected from projectors induced high electric field gradients locally at illuminated spots. This method was demonstrated to form virtual walls, guiding particles or cells flowing through pre-designed paths using the negative dielectrophoresis (nDEP) forces (Lu *et al.* 2004a). The positive dielectrophoresis (pDEP) forces were also generated to attract and to trap yeast cells (Lu *et al.* 2004b). This image dielectrophoresis (iDEP) method does not require masking fabrication process used in the cDEP. The iDEP produces lower optical intensity by 1000 times compared to optical tweezer, reducing damage on cells.

Still, the iDEP is premature to be practically used in cell manipulation. The previous developments in the last two years mainly focus on moving particles or cells toward location of desire. In this study, the controllability of cell manipulation using the iDEP will be analyzed. The parameters of the controllability to be characterized include the affinity of cells in different conductivity solutions and the effective work region of image patterns.

The iDEP is a derivation of cDEP except the electric field gradient induced optically. The iDEP force can still be expressed using the cDEP formula as in Equation (1).

$$F_{\mathrm{DEP}} = 2\pi a^3 \varepsilon_m \mathrm{Re}[K^*(\omega)]\nabla(E^2), \tag{1}$$

where a, ε_m, E and $K^*(\omega)$ are cell radius, permittivity of surrounding media, electric field and clausius-mositti factor. The $K^*(\omega)$ can be further shown as

$$K^*(\omega) = \frac{\varepsilon_p^* - \varepsilon_m^*}{\varepsilon_p^* + 2\varepsilon_m^*} \tag{2}$$

where ε^* is complex permittivity (i.e. $\varepsilon^* = \varepsilon - j(\sigma/\omega)$); σ is the conductivity; ω is the electric field frequency. The subscripts p and m denote particles and the surrounding media, respectively. The cDEP utilizes ac voltage bias between electric plates to induce non-uniform electric fields. In response to the electric fields applied, the polarizable cells are guided to the places with higher electric fields. This phenomenon (i.e. $\mathrm{Re}[K^*(\omega)] > 0$) is named as positive dielectrophoresis; on the contrary, nDEP is called for the condition of $\mathrm{Re}[K^*(\omega)] < 0$.

2. System

Figure 1 shows the setup of a typical iDEP system, including a programmable light source, a sample chip and a monitoring system. The programmable light source used was a 1200 lm commercial TFT-LCD projector to produce flash images that were generated and controlled by a computer. Different image patterns were edited using Flash MX®. Users can move the designed images, such as square patterns and cursors, through PC mouses. A CCD camera connected to the computer was installed to capture cells' behaviors and projected image patterns. The sample chip was comprised of two ITO (Indium-Tin-Oxide) glass chips with a 50 μm spacer in between. Cells and liquid solutions were confined in the sample chip. The bottom ITO glass was deposited with amorphous silicon (α-Si) on top as a photoconductor layer. When ac voltages were applied across the two ITO glasses, uniform electric fields were formed and no DEP forces were produced on cells. The gradients of the electric fields become higher at illuminated regions because photovoltaic effects on the amorphous silicon layer due to illumination enhance electrical conductivities locally. Each optical pixels projected on the chips were measured to be 25 μm by 25 μm. The overall usable areas of each projected images was characterized to be about 20 mm by 15 mm.

3. Experimental results and discussion

The cell species tested in the study were viable yeast. The DEP affinity and the effective DEP radius (R_{eff}) were investigated to analyze the manipulation controllability of the iDEP method. The viability of cell was tested using dying method after iDEP manipulation. The viability of cell indicates the biocompatibility of the iDEP technology.

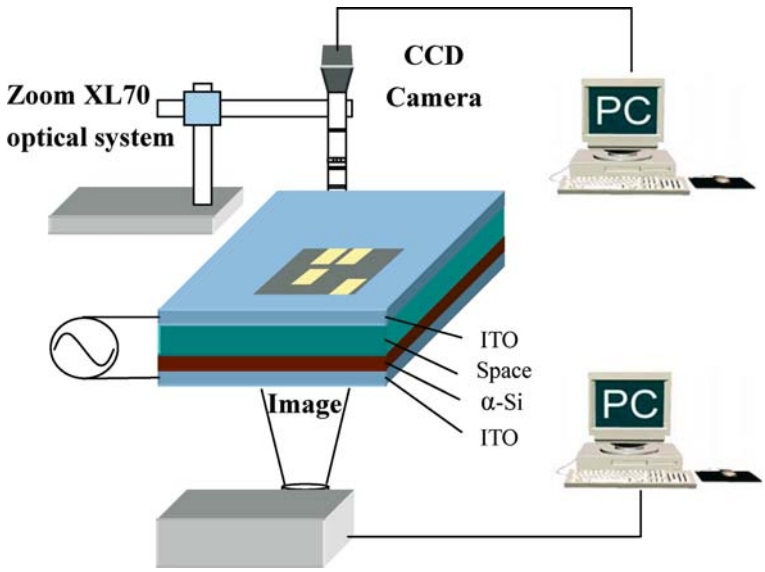

Fig. 1. System schematic of image dielectrophoretic technique.

3.1. CELL DEP AFFINITY

To characterize the cell DEP affinity, liquid conductivities and ac frequencies were adjusted. The solutions mixed of NaCl and DI water had the conductivities varying from 4 μS/cm to 600 μS/cm. The ac frequencies were adjusted from 10 Hz to 10 MHz. The yeast cells were first immersed in the pre-mixed solutions and were then injected into sample chips. The DEP affinities of the yeast cells with respect to ac frequencies of 10 V_{pp} and to solution conductivities were listed in Table 1. The DEP affinities were qualitatively distinguished either as pDEP or as nDEP based on the motion direction of the cells under non-uniform electric fields.

Table 1 shows that the yeast cells have detectable DEP affinity under the ac frequencies below 100 kHz and solution conductivities below 450 μS/cm.

Table 1. The affinity test of the yeast cells in different conductivity of solutions

Conductivity (μS/cm)	Frequency (Hz)						
	10	100	1 K	10 K	100 K	1 M	10 M
4	–	+	+	+	+	×	×
150	0	+	+	+	+	×	×
300	0	×	×	+	+	×	×
450	0	0	×	+	+	×	×
600	0	0	0	×	×	×	×

+: Positive DEP force; –: Negative DEP force; ×: No response; 0: Electrolysis.

As the liquid conductivity increases from 4 μS/cm to 600 μS/cm, the DEP behaviors vanish. This phenomenon can be obtained from Equations (1) and (2) given negligible conductivity of the cells. The real part of the clausius-mositti factor can be expressed as

$$\mathrm{Re}[K^*(\omega)] \propto \varepsilon_p^2 + \varepsilon_p \varepsilon_m - 2\varepsilon_m^2 - 2(\sigma_m/\omega)^2. \tag{3}$$

The real part of the clausius-mositti factor approaches zero when the liquid becomes more conductive in the test.

3.2. EFFECTIVE DEP RADIUS

In addition to the DEP affinities of the yeast cells, the effective DEP radius was also measured to analyze the range within that the DEP forces have detectable influence on the cells (see Fig. 2). The cells' motions were characterized when the square images of four pixels were projected onto the chips. The effective DEP radius is defined as the farthest boundary where cell velocities exceed 25 μm/min (i.e. over one pixel per minute in this study).

The effective DEP radius was measured with respect to ac voltages and frequencies. Table 1 indicates that the yeast cells have pDEP affinity at the ac frequencies of interest (e.g. 1 kHz and 10 kHz). The pDEP force attracted the yeast cells toward illuminated areas. According to recorded one-minute video clips, the effective radius was determined from the center

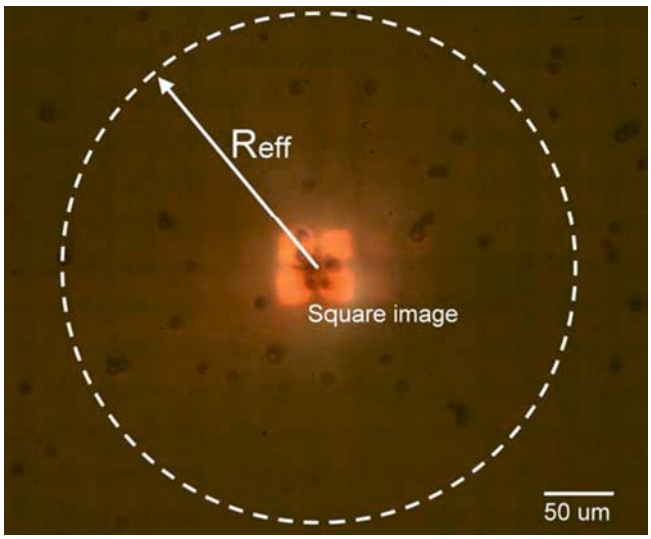

Fig. 2. The effective DEP radius (R_{eff}) of the iDEP manipulation.

of the square image to the distance where the cells move by no more than 25 μm (i.e. one pixel of the images). Figure 3 reveals the experimental results of the effective DEP radius for the yeast cells in 4 μS/cm solutions. The effective DEP radius increased as ac voltages became larger. At 10 V_{pp}, the effective DEP radius exceeded 475 μm and 425 μm for 1kHz and 10KHz, respectively. This result agreed with the implication of Equation (1). The DEP force increases proportionally to voltage applied; thus, the effective DEP radius become larger.

The effective DEP radius, on the other hand, can be reckoned as the distance from the center of the images projected where the DEP force equals to the drag force on the cells. The minimum detectable velocity of the cells was defined as 25 μm/min for determination of cell immobility; the velocity was constrained by the detection capability of the system. The drag force in laminar flows can be expressed as in Equation (4) from Stoke's law.

$$F_{\text{drag}} = 6\pi\mu av, \tag{4}$$

where μ is the viscosity of liquid solutions. The viscosity of the DI water is $1 \times 10^{-3}\text{N}\times\text{s/m}^2$ at 20°C (Young *et al.* 2001). The drag force is linearly proportional to the viscosity, the radius of cells and the velocity of cells. Given the minimum detectable cell velocity of 25 μm/min and the yeast cells of about 5 μm in diameter, the DEP force induced was estimated to be 20 fN.

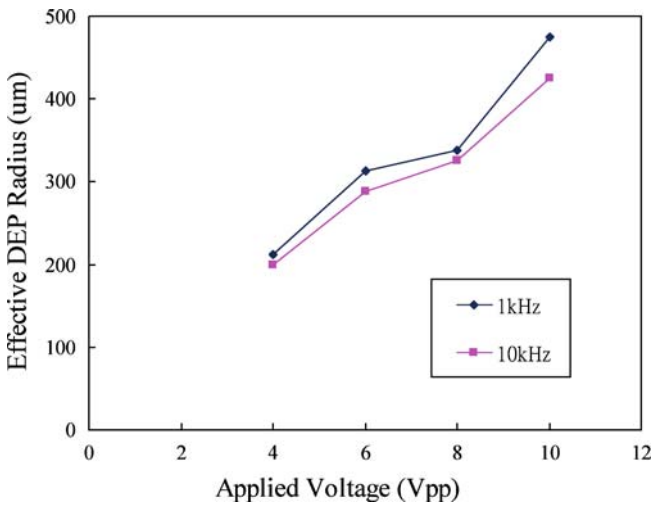

Fig. 3. The relationship between the effective DEP radius and applied voltage.

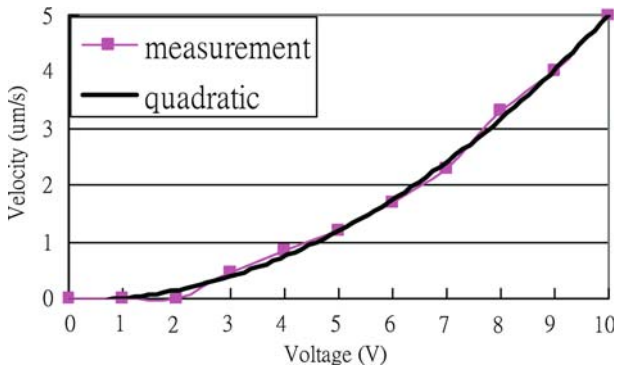

Fig. 4. The measured cell velocity versus ac voltage applied.

3.3. THRESHOLD VOLTAGE

Cells' velocities nearby the illuminated spots were also measured for different voltage biases applied at 100 Hz shown in Fig. 4.

The velocities were found to be in a good agreement with (5), implying velocities proportional to square of the voltage applied minus a threshold voltage. Equation (5) was derived from (1) based on the conservation of momentum and $E \propto V$.

$$F(\nabla(V^2))\Delta t = m\Delta v. \tag{5}$$

The best-fit relation of velocity to voltage could be expressed as in Equation (6).

$$v = 0.05 \times V^2. \tag{6}$$

The threshold voltage was measured to be 3 V for the cells to initiate their motions at the minimum detectable cell velocity of 25 μm/min. The corresponding static friction to overcome was estimated to be 20 fN from Equation (4). When voltages applied were lager than threshold voltage, the cells' velocities increase proportionally to the voltage squared and finally reached 5 μm/s at 10 V.

3.4. PARALLEL MANIPULATION

To achieve parallel manipulation, it is of users' desire to move cells at the fastest velocities as well as to have minimum influence on the cells of no interest. There exists trade off between the cell velocities and the effective DEP radius. When ac voltage bias decreases, the effective DEP radius

shrinks and the cell velocity nearby illuminated spots also slows down. Combination of Equations (1) and (4) yields (7).

$$\frac{\nabla(E^2(\text{spot}))}{\nabla(E^2(R_{\text{eff}}))} = \frac{v(\text{spot})}{v(R_{\text{eff}})}, \tag{7}$$

where $\nabla(E^2(\text{spot}))$ and $\nabla(E^2(R_{\text{eff}}))$ denote the gradient of the electric field at the edges of the illuminated spots and at the boundaries of the effective DEP radius, respectively. $v(\text{spot})$ and $v(R_{\text{eff}})$ represent the velocities at the spot edges and at the effective DEP boundaries, respectively. The left-hand side of Equation (7) depends on the geometric patterns of the projected images. Assign $v(R_{\text{eff}})$ equal to the minimum detectable velocity, implicitly yielding $R_{\text{eff}}/v(\text{spot}) = \text{constant}$. To obtain faster cell motions also results in larger effective DEP radius. It is desired to conduct efficient parallel manipulation under appropriate ac signals that must satisfy the requirements of larger than the threshold voltage and the effective DEP radius equal to the range of desire.

An experimental result of sequential parallel manipulation was shown in Fig. 5. Four square patterns of 100 μm by 100 μm were projected onto the chip. The initial spacing between two adjacent squares was measured to be about 125 μm. The ac signals applied to the chips was 10 V_{pp} at 10 kHz in the experiment. In Fig. 5, the upper right spot moved toward the right at 1.6 μm/s. The cells were confined within the spot and moved along with it. Furthermore, the cells confined in the other three light spots remained intact.

3.5. CELL VIABILITY

After the experiment of the parallel manipulation, dying reagent, 0.4% Trypan blue, was used for testing the viability of yeast cells. The viable cells were dyed blue only at cell membranes by the reagent and still transparent in the center. If cells were non-viable, the reagent would immerse into cells and make the whole cells blue. According to a colorimeter, two plunged peaks of red and green primary colors showed at boundary of the cell as shown in Fig. 6(a). This is evidence that cells still kept their viability, after iDEP manipulation. A control experiment (see Fig. 6(b)) was done by burning yeast cells under hot water at 100°C for 10 min. Figure 6(b) shows only one plunged peak at the center of cells because of the immersed blue reagent.

4. Conclusion

Compared to mechanical manipulators and optical tweezers, the iDEP has advantages of non-contact cell manipulation and 1000X lower optical

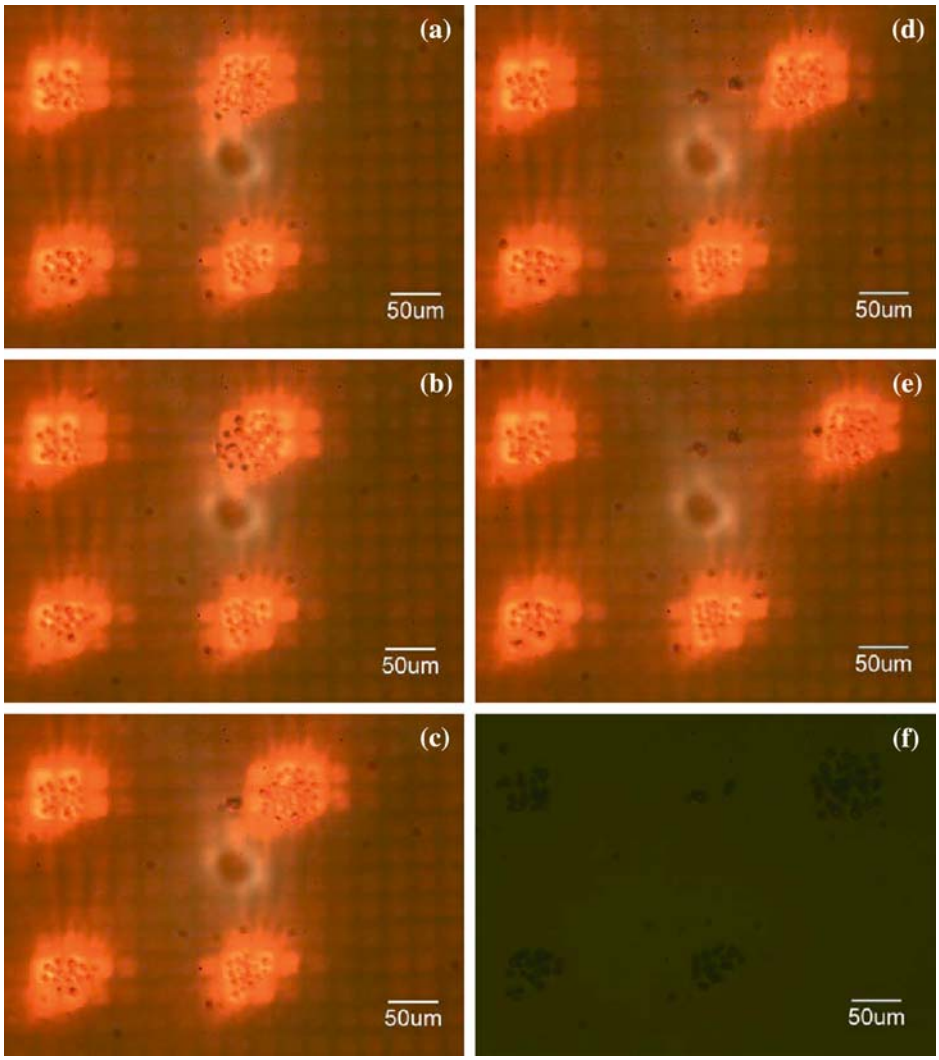

Fig. 5. Influence study of four independent illuminated spots on cells' motions. A sequence of six images (a)–(f) shows one illuminated spot moved toward right and the rest stayed stationary. The yeast cells were included in the top-right spot and moved along with the spot.

power intensity, intended for negligible damage to cells. Influences of images patterns were characterized at various ac frequencies and liquid conductivities. DEP affinities of cells, effective DEP radius and threshold voltages were determined for the controllability of the iDEP. Parallel manipulation was, thus, demonstrated based on the analyzed DEP information. The parallel manipulation of the cells permits users to simultaneously control many cells independently and still keeps cells viability. In addition,

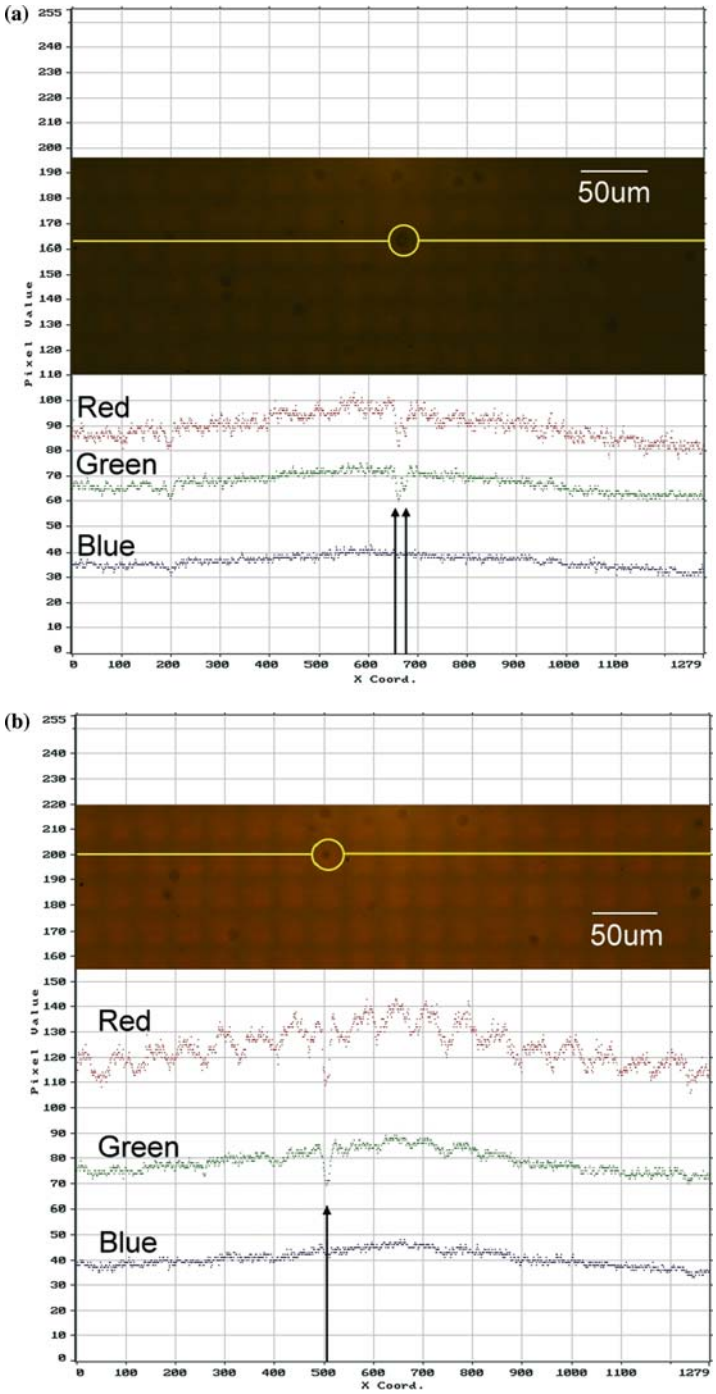

Fig. 6(a). The measurement results of cell viability by a colorimeter. (a) Viable cells show two plunged peaks at cell membranes. (b) Non-viable cells only got one plunged peak at the center because of the immersed blue reagent.

this study can be further applied to produce cell reservoirs to temporarily store cells by projecting desired image patterns on the chips.

Acknowledgements

The authors are indebted to Shu-Chuan Lin who is currently a Ph.D. student of Institute of Molecular and Cellular Biology at National Tsing Hua University for her technical assistance in cell preparation.

References

Ashkin, A. and J.M. Dziedzic. *Appl. Phys. Lett*. **19** 283, 1971.
Ashkin, A., J.M. Dziedzic, J.E. Bjorkholm and S. Chu. *Opt. Lett.* **11** 228, 1986.
Ashkin, A. *J. Sel. Top. Quant. Electron.* **6** 841, 2000.
Chiou, P.Y., Z. Chang and M.C. Wu. In: *Proceeding of IEEE/LEOS International Conf. Optical MEMS, 18–21 August 2004,* 8, 2003.
Curtis, J.E., B.A. Koss and D.G. Grier. *Opt. Commun.* **207** 169, 2002.
Das, M., F. Chandra, F. Becker, S. Vernon, J. Noshari, C. Joyce and P.R.C. Gascoyne. *Anal. Chem.* **77** 2708, 2005.
Jager, W., H. Edwin, O. Inganas and I. Lundstrom. *Science* **288** 2335, 2000.
Li, Haibo, Bashir and Rashid, *Sens. Actuators B* **86** 215, 2002.
Lu, Y.S., Y.H. Chang, S.P. Tseng and J.A. Yeh. In: *Proceeding of IEEE/LEOS International Conf. Optical MEM, 22–26 August 2004,* 20, 2004a.
Lu, Y.S., Y.P. Huang, J.A. Yeh and C. Lee. In: *Proceeding of the Second Asian and Pacific Rim Symposium on Biophotonic, 14–17 December 2004,* 238, 2004b.
Neuman, K.C., G.F. Liou, S.M. Block and K. Bergman. In: *Lasers and Electro-Optics Europe, (CLEO 1998) Technical Digest. Summaries of papers presented at the Conference, 14–18 September 1998*, 203,1998.
Ohta, A.T., P.T. Chiou and M.C. Wu. In: *Proceedings of Solid State Sensor, Actuator and Microsystems Workshop (Hilton Head 2004), 6–10 June 2004,* 216, 2004.
Pohl, H.A. *J. Appl. Phys.* **22** 869, 1951.
Pohl, H.A. *Dielectrophoresis*. Cambridge University Press, 1978.
Sachiko, O., Y. Tomoyuki and M. Tomokazu. *Bioelectrochem.* **54** 33, 2001.
Wang, X.B., Y. Huang, J.P.H. Burt, G.H. Markx and R. Pethig. *J. Phys. D* **26** 1278, 1993.
Wang, X.B., M.P. Hughes, Y. Huang, F.F. Becker and P.R.C. Gascoyne. *Biochim. Biophys. Acta.* **1243** 185, 1995.
Wu, Z., B. Wang, K. Shao and S. Akio. *Colloids Surf. B* **11** 273, 1998.
Yang, J., Y. Huang, X.B. Wang, F.F. Becker and P.R.C. Gascoyne. *Anal. Chem.* **71** 911, 1999.
Young D.F., B.R. Munson and T.H. Okiishi. *A brief information to fluid mechanics*, 2nd edn., Wiley, 2001.